

Spectral Descriptors for Graph Matching

Nan Hu Leonidas Guibas
Stanford University
Stanford, CA, USA

nanhu@stanford.edu, guibas@cs.stanford.edu

Abstract

In this paper, we consider the weighted graph matching problem. Recently, approaches to this problem based on spectral methods have gained significant attention. We propose two graph spectral descriptors based on the graph Laplacian, namely a Laplacian family signature (LFS) on nodes, and a pairwise heat kernel distance on edges. We show the stability of both our descriptors under small perturbation of edges and nodes. In addition, we show that our pairwise heat kernel distance is a noise-tolerant approximation of the classical adjacency matrix-based second order compatibility function. These nice properties suggest a descriptor-based matching scheme, for which we set up an integer quadratic problem (IQP) and apply an approximate solver to find a near optimal solution. We have tested our matching method on a set of randomly generated graphs, the widely-used CMU house sequence and a set of real images. These experiments show the superior performance of our selected node signatures and edge descriptors for graph matching, as compared with other existing signature-based matchings and adjacency matrix-based matchings.

1 Introduction

Graph matching techniques have been widely used in computer vision such as 2D [?, ?] and 3D [?] image analysis, biomedical identification [?, ?], and object tracking over video sequences [?, ?]. Most of the algorithms used in practice belong to the category of inexact matching where people consider graphs with noise. In this paper we consider the problem of graph matching for weighted undirected graphs with noise. These kind of graphs appear commonly in computer vision when objects in images undergo either rigid or deformable motion.

In this paper we propose to use spectral descriptors as first and second order compatibility functions in an integer quadratic programming (IQP) setting. Spectral methods [?, ?, ?, ?, ?, ?] have been widely used in graph matching algorithms because of the fact that the graph adjacency matrix and its derivatives are spectrally invariant under permutations. Recently, spectral node signatures have drawn significant attention for shapes, e.g. the heat kernel signature (HKS) [?] and the wave kernel signature (WKS) [?]. Inspired by the common structure of HKS and WKS, we propose in this work a generic one-parameter family of node signatures based on the graph Laplacian and generalizing the HKS and WKS, which we call the Laplacian family signatures (LFS). This generic structure permits other spectral node signatures to be easily generated. In addition, we unify the stability of HKS and WKS under small perturbations of the graph into our LFS framework.

Besides the use of LFS as the first order compatibility condition, we propose to define a pairwise heat kernel distance as a second order condition. We show in the paper that the pairwise heat kernel distance is a noise-tolerant approximation to the classical pairwise adjacency distance, which is often used as the second order compatibility function [?].

Setting LFS as the first order compatibility condition and pairwise heat kernel distance as the second order compatibility condition, we formulate the graph matching problem as a general IQP. We use the approximate solver proposed recently by Cho et. al. [?] — a reweighted random walk matching algorithm that has shown superior performance over other state-of-the-art IQP solvers. We test our spectral descriptors on three different graph matching experiments, i.e. randomly generated graphs, CMU house sequence, and real images. Our proposed descriptors are more robust than the classical adjacency matrix based matching.

The rest of the paper is organized as follows. In Section 1.1, we review previous work on graph matching that is related to our proposed descriptors. We introduce our spectral descriptors and their properties in Section 2. The descriptors are then used as compatibility functions and set up as IQP in Section 3. Last but not the least, we present our experimental results in Section 4 before the paper is concluded in Section 5

1.1 Related Work

Node-based signatures have been used on graphs, both inside and out of matching. Joilli et. al.[?] proposed a signature composed of the degree of the a node followed by the ordered weights of each incident edge and padded with zero if necessary. Gori et. al. [?] constructed node signatures from the steady state distributions of simulated random walks similar to PageRank. Eshera [?] built signatures for attributed relational graphs (ARG). Shokoufandeh et. al [?] constructed feature-based node signatures for bipartite matching. The same authors [?] later proposed a topological signature vector (TSV) for directed acyclic graphs (DAG). Outside of graph matching, Wong et. al [?] proposed a topological signature. Their signature is constructed as a local histogram of the number of nodes.

Our signature is also related to spectral method in graph matching. Among the pioneering work of spectral method is Umeyama’s [?] weight graph matching algorithm. His method was later generalized to graphs of different size [?, ?]. Robles-Kelly et. al. [?] ordered the nodes from the steady state of markov chain with the edge connectivity constraint and matched using edit distance. In their 2005 paper [?], node ordering was done using the leading eigenvector of the adjacency matrix. Qiu et. al [?] considered using Fiedler vector to partition the graph for a hierarchical matching. Their method, however, works only on planar graphs. Cho et. al. [?] constructed a reweighed random walks similar to personalized PageRank on the association graph with the addition of an absorbing node. They computed the quasi-stationary distribution and discretize the continuous solution to find a matching. Emms et. al. [?] built an auxiliary graph from the two graphs and simulate a quantum walk. Particle probability of each auxiliary node is used as the cost of assignment for a bipartite matching.

In a broader sense of relatedness to our work is other relaxation-based matching algorithms. Gold and Rangarajan [?] proposed the well-know *Graduated Assignment Algorithm*. van Wyk et. al. [?] designed an projection onto convex set (POCS) based algorithm to solve IQP by successively project the relaxation solution onto the convex constraint set. Schellewald et. al. [?] constructed a semidefinite programming relaxation of the IQP. Leordeanu et. al. [?] proposed a spectral method to solve a relaxed IQP where they drop off the linear inequality constraint during relaxation and only incorporate it at the discretization step. The idea was further extended by Cour et. al. [?], where they added an affine constraint during relaxation. Zaslavskiy et. al. [?] approached the IQP from the point of a relaxation of the original least-square problem to a convex and concave optimization problem on the set of doubly stochastic matrices. Leordeanu et. al. [?] proposed an integer projected fixed point (IPFP) algorithm to solve the quadratic assignment problem.

2 Graph Spectral Descriptors

In this section, we will introduce the Laplacian family signatures (LFS) as graph node descriptor and the heat kernel as the graph edge descriptor and their properties.

2.1 Preliminary on Graph Laplacian

Let the undirected graph under discussion be denoted by $G = (V, E)$, where V is the set of vertices, and $E \subseteq V \times V$ is the set of edges. Let w be the weights on edges, i.e. $w : E \mapsto \mathbb{R}^+$. The graph Laplacian is defined as $\mathcal{L} = D - A$, where A is the graph adjacency matrix with

$$A_{ij} = \begin{cases} w(i, j) & \text{if } (i, j) \in E \\ 0 & \text{otherwise} \end{cases}$$

and D is a diagonal matrix of total incident weights, i.e. $D_{ii} = \sum_j A_{ij}$.

\mathcal{L} is symmetric and positive semi-definite and has non-negative eigenvalues, the smallest of which is 0 and the multiplicity equals the number of connected components.

Similar to classical Fourier transform, where complex exponentials $e^{i\omega x}$ are the eigenfunctions of Laplacian operator $\frac{d}{dx^2}$, eigenvectors of \mathcal{L} can be used to define the graph Fourier transform [?]. In that sense, if (λ_i, ϕ_i) are the eigenpairs of \mathcal{L} , λ_i are discrete frequencies and ϕ_i are eigenfunctions of each frequency.

2.2 Laplacian Family Signatures

Definition 1. For a graph G with laplacian \mathcal{L} , if (λ_i, ϕ_i) are the eigenpairs of \mathcal{L} , then the LFS $s_l(t)$ of node $l \in V$ is defined as

$$s_l(t) = \sum_k h(t; \lambda_k) \phi_k(l)^2,$$

where $h(t; \lambda_k)$ is called the construction kernel.

Choosing $h(t; \lambda_k) = \exp(-t\lambda_k)$ results in the heat kernel signature (HKS) [?], where the authors have shown the multi-scale and informative properties on manifolds with application on shape analysis. HKS came from the simulated heat diffusion process. For each node, the signature captures the amount of heat left at the node at various time slices when a unit amount is put on the node initially. While selecting $h(t; \lambda_k) = \exp(-\frac{(t - \log \lambda_k)^2}{2\sigma^2})$, it becomes the wave kernel signature (WKS) [?]. WKS came from the natural counterpart of heat diffusion, the particle quantum process. The signature captures the particle distribution probability at different energy band. If assuming $h(t; \lambda_k) = g(t\lambda_k)$ is band-pass with special behavior at origin, the kernel becomes wavelet kernel [?] which could be easily extended within our generic framework to wavelet signature.

The family of signatures are intrinsic, namely they are invariant under isomorphism. Besides, one important property of LFS is its stability under small perturbations. HKS and WKS have been shown to be stable in their original work. Inspired from them, we unify the stability to LFS and extend it to Laplacians with repeated eigenvalues. (see supplementary material for the proof).

Theorem 1 (LFS Continuity). Let \mathcal{L} be the laplacian of a graph, and \mathcal{L}' be a perturbed laplacian. Let the size of the graph be n , and $\lambda_1 < \dots < \lambda_k$ denote the k distinct eigenvalues of \mathcal{L} . Let $s_i(t)$ and $s'_i(t)$ denote the LFS's of node i . If $\lambda_{j+1} - \lambda_j \geq \delta, \forall j$, $\|\mathcal{L} - \mathcal{L}'\|_F \leq \epsilon < \delta$, and $h(\cdot; \cdot) \in C^2(\mathbb{R}_+^2)$, then if $k = n$, we have

$$|s'_i(t) - s_i(t)| \leq C_0(\delta, t)\epsilon,$$

where $C_0(\delta, t)$ is a constant independent of ϵ , and if $k < n$ we have

$$|s_i(t) - s'_i(t)| \leq C_1(t) \left(\frac{\delta}{\delta - \epsilon} - 1 \right) + C_2(t)\epsilon,$$

where $C_1(t), C_2(t)$ are constants depends only on t .

When the number of nodes are different, we could use lifting ideas similar to [?] to prove its stability.

To better illustrate the stability of LFS, Fig. 1a showed the WKS of all the nodes from a randomly generated graph with 5 nodes and perturbed counterparts.

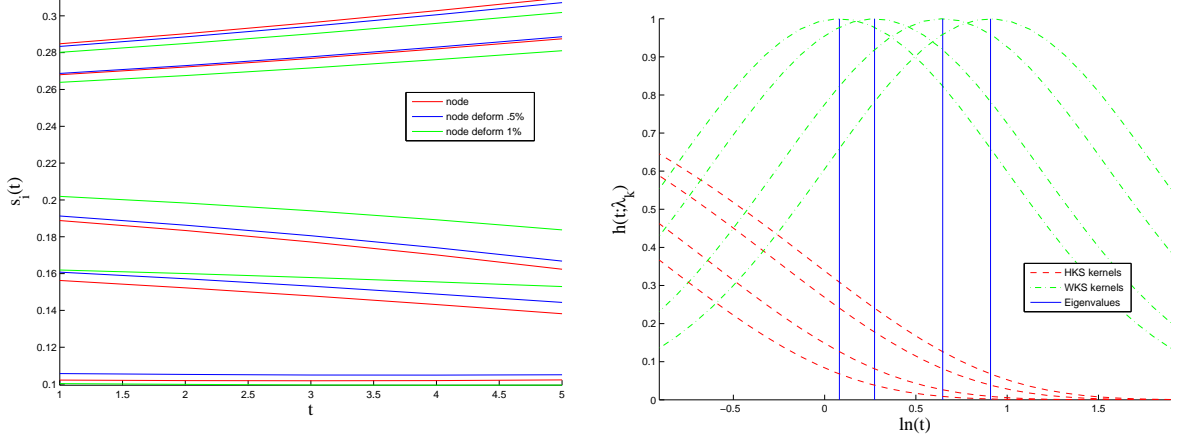
There are two signature distances defined in [?] and [?] respectively.

Definition 2. Let $t_{\min} = t_0 < t_1 < \dots < t_s = t_{\max}$ be discrete samples. Let $s_i(t)$ and $s_j(t)$ be two LFS. Then the relative L_1 distance [?] between two LFS is defined as

$$d_1(i, j) = \sum_{k=0}^L \frac{|s_i(t_k) - s_j(t_k)|}{s_i(t_k) + s_j(t_k)},$$

and the L_2 distance [?] is defined as

$$d_2(i, j) = \left(\sum_{k=0}^s |s_i(t_k) - s_j(t_k)|^2 \right)^{\frac{1}{2}}.$$



(a) WKS for a randomly generated graph of 5 nodes and when perturbed.

(b) HKS and WKS kernels for a randomly generated graph.

Figure 1: Perturbation of WKS and Illustration of HKS/WKS kernels.

L_2 distance reflects more the absolute difference upon each time slice t , while relative L_1 distance that concentrates more on the relative difference on each t .

Within the family of signature, nevertheless, HKS and WKS are representative of two categories, namely, *coupled* and *decoupled* LFS. The significance of coupling to matching performance is shown in Section 4.

Definition 3. A coupled LFS admits a construction kernel of the form

$$h(t; \lambda_k) = \mu(t\lambda_k)$$

for some function $\mu(\cdot)$.

An LFS is called *decoupled* if it is not coupled. Wavelet signature, therefore, is another realization of coupled LFS.

The coupling of parameters t and λ_k is one of the major differences in HKS and WKS as pointed out in [?] that would affect their matching accuracies (as shown in Section 4). Fig. 1b showed the construction kernel of HKS and WKS for a randomly generated graph with 5 nodes. The *decoupled* WKS kernel makes the sampling more effective as for each discrete frequency (eigenvalue), there is a kernel which is dominating all other kernel within a small neighborhood around that frequency and as a result each frequency is well represented in the signature. While for the *coupled* HKS kernel, one kernel ($\exp(-t\lambda_1)$) uniformly dominates all other kernels over the domain, which makes high frequency components less and less representative in the signature.

On the other hand, the Gaussian function used in WKS kernel per se is locally flat at the origin (first order derivative is zero), and therefore more tolerant to eigenvalue perturbations.

2.3 Heat Kernel

In this section, we will introduce the concept of heat kernel. The heat diffusion process on graph G is governed by the heat equation $\mathcal{L}u(t) + \frac{\partial}{\partial t}u(t) = 0$, where $u(t) \in \mathbb{R}^{|V|}$ is the heat distribution vector, and \mathcal{L} is the graph laplacian. Given an initial heat distribution $f : V \mapsto \mathbb{R}^{|V|}$, let $\mathcal{H}_t(f)$ be the heat distribution at time t . \mathcal{H}_t is called the heat operator and can be expressed as $\mathcal{H}_t = e^{-t\mathcal{L}}$. Both \mathcal{L} and \mathcal{H} are linear operators mapping real-valued functions defined on vertices of graph to another such function, and they share the same eigenvalues.

Similar to heat diffusion on manifold, there is also a heat kernel on graph, which satisfies $\mathcal{H}_t f(x) = \sum_{y \in V} k_t(x, y) f(y)$. $k_t(x, y)$ can be think of as the amount of heat transferred from node x to node y at time t when unit amount is put on x at $t = 0$. The heat kernel has the following eigen-decomposition

$$k_t(x, y) = \sum_{i=1}^{|V|} \exp(-t\lambda_i) \phi_i(x) \phi_i(y),$$

Stability of $k_t(x, y)$ can be shown similar to that of LFS in section 2.2.

$k_t(x, y)$ is a low-pass filter on graph analogously to that in signal processing. If we write heat kernel $\mathcal{K}_t = \sum_i \exp(-t\lambda_i) \phi_i \phi_i^\top$, for any initial distribution $f \in \mathbb{R}^{|V|}$, noticing that $\hat{f}(i) = \phi_i^\top f$ is the Fourier coefficient, $\mathcal{H}_t f = \mathcal{K}_t f = \sum_i \exp(-t\lambda_i) \hat{f}(i) \phi_i$. For a fixed t , the scaling function $\exp(-t\lambda_i)$ suppresses high frequencies and hence \mathcal{K}_t has a low-pass effect. t in that sense controls the pass-band, namely as t increases, passband decreases.

Definition 4. Let k_t and k'_t be two heat kernels of $G = (V, E)$ and $G' = (V', E')$. For $i, j \in V$ and $a, b \in V'$, the pairwise heat kernel distance is defined as

$$d_t^K(i, j, a, b) = |k_t(i, j) - k'_t(a, b)|,$$

and the pairwise adjacency distance is

$$d^A(i, j, a, b) = |A(i, j) - A'(a, b)|.$$

The pairwise heat kernel distance d_t^K is noise-tolerant approximation of pairwise adjacency distance d^A (see supplementary material for a proof).

Theorem 2 (Noise Tolerant Approximation). Let $d_t^K(i, j, a, b)$ and $d^A(i, j, a, b)$ be the pairwise heat kernel distance and pairwise adjacency distance for graph G and G' . Let λ_i and λ'_i be the set of eigenvalues of G and G' .

$$\lim_{t \rightarrow 0} \frac{d_t^K(i, j, a, b)}{t} = d^A(i, j, a, b),$$

and

$$\sum_{i \neq j} \sum_{a \neq b} (d_t^K(i, j, a, b))^2 \leq \sum_i \exp(-2t\lambda_i) + \sum_i \exp(-2t\lambda'_i)$$

For small t , d_t^K is a good approximate of d^A . As t increases, d_t^K is smoothed out. Therefore it starts from a good approximation to d^A , and the differences in d^A was smoothed away in d_t^K as t increases. That way, it becomes noise tolerant, because ideally without noise d^A would be zero everywhere for matched pairs.

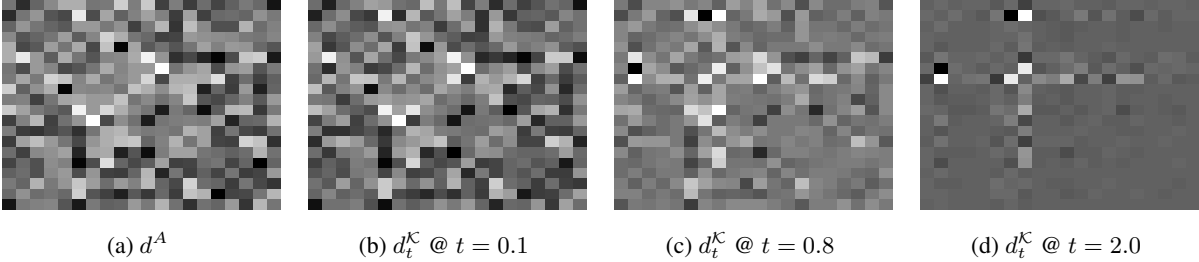


Figure 2: d_t^K at different time and comparison with d^A .

Fig. 2 illustrated an example of this smoothing effect on a noisy pair of graphs. When t is small, d_t^K is a well approximate of d^A . While when t goes large the difference in d_t^K is smoothed away.

3 Matching Scheme

To compare the performance within LFS and with other node signatures, the problem is cast as a bipartite graph matching problem as in existing node signature based matching work [?, ?, ?], where costs are set as the distance between signatures (d_2 for HKS and d_1 for WKS). The problem is solved by the well-known Hungarian algorithm [?] in the complexity of $O(n^3)$, where n is the size of the larger graph.

In addition to node signatures, we could include pairwise heat kernel distance d_t^K as the second order constraint and formulate the problem in an integer quadratic program (IQP) setting.

For two graphs $G = (V, E)$ and $G' = (V', E')$. Let $d(i, a)$ be the distance between their node signatures. We construct a compatibility matrix $W \in \mathbb{R}^{|V||V'| \times |V||V'|}$ as

$$W_{ia,jb} = \begin{cases} d_t^K(i, j, a, b) & i \neq j, a \neq b \\ \alpha d(i, a) & i = j, a = b \end{cases}$$

If $\mathbf{X} \in \{0, 1\}^{|V||V'|}$ be the one-to-one mapping matrix and $\mathbf{x} \in \{0, 1\}^{|V||V'|}$ is the vector form of \mathbf{X} . The IQP could be written as

$$\begin{aligned} \mathbf{x}^* &= \arg \min(\mathbf{x}^\top W \mathbf{x}) \\ \text{s.t. } \mathbf{x} &\in \{0, 1\}^{|V||V'|}, \forall i \sum_{a \in V'} \mathbf{x}_{ia} \leq 1, \forall a \sum_{i \in V} \mathbf{x}_{ia} \leq 1 \end{aligned}$$

As is well-known that this problem is NP-complete and there are a whole literature of approximation algorithms. Comparison of the performance of different IQP approximation solvers is outside the scope of our paper. In our experiment, we selected a recently proposed algorithm, reweighed random walk matching (RRWM) [?]. The main reason we chose this algorithm is the superior performance they have shown compared with other state-of-the-art approximation algorithm, including SM [?], SMAC [?], HGM [?], IPFP [?], GAGM [?], SPGM[?]. For the completeness of our presentation, we list a pseudocode of their algorithm in Algorithm 1 and left details to their original paper.

Algorithm 1 RRWM [?]

- 1: Given compatibility matrix W , reweight factor α , inflation factor β ,
 - 2: Set $W_{ia,jb} = 0$ for conflicting matchings,
 - 3: Compute $d_{max} = \max_{ia} \sum_{jb} W_{ia,jb}$,
 - 4: Initialize transition matrix $P = W/d_{max}$, and \mathbf{x} uniform,
 - 5: **repeat**
 - 6: $\mathbf{x}^\top = \mathbf{x}^\top P$,
 - 7: $\mathbf{y}^\top = \exp(\beta \mathbf{x} / \max \mathbf{x})$,
 - 8: **repeat**
 - 9: Normalize rows, $\mathbf{y}_{ia} = \mathbf{y}_{ia} / \sum_a \mathbf{y}_{ia}$,
 - 10: Normalize columns, $\mathbf{y}_{ia} = \mathbf{y}_{ia} / \sum_i \mathbf{y}_{ia}$,
 - 11: **until** \mathbf{y} converges
 - 12: $\mathbf{y} = \mathbf{y} / \sum \mathbf{y}_{ia}$,
 - 13: $\mathbf{x}^\top = \alpha \mathbf{x}^\top + (1 - \alpha) \mathbf{y}^\top$,
 - 14: $\mathbf{x} = \mathbf{x} / \sum \mathbf{x}_{ia}$,
 - 15: **until** \mathbf{x} converges
 - 16: Discretize \mathbf{x} .
-

4 Experiments

We tested our descriptor on three different datasets: 1. synthetically generated random graphs; 2. CMU House sequence for point matching; 3. Feature matching using real images.

4.1 Sythetic Random Graphs

In this section, follow the experimental protocol of [?], we synthetically generate random graphs and perform a comparative study. In the first part of the experiment, we use random graphs from Erdos-Rényi model $G(n, m)$. For each selected edge, we add a uniform $[0, 1]$ random weight. The graph is then perturbed by adding random Gaussian noise $\mathcal{N}(0, \sigma^2)$ on selected edges.

In this test, we compare the performance within our LFS and with existing nodes signatures, namely degree vector signature (DVS) [?], local histogram signature (LHS) [?], random walk signature (RWS) [?]. Although HKS and

WKS are the only existing LFS known in the literature, it is not difficult to construct LFS using other form of kernels. Noticing that both HKS and WKS kernels are continuous probability density functions (pdf) for some distribution, we generalize them to other form of continuous pdf's: 1. Gamma kernel $(t\lambda_i)^{k-1} \exp(-t\lambda_i/\theta)$, 2. Gaussian kernel $\exp(-(t - \mu(\lambda_i))^2/2\sigma^2)$, 3. Laplacian kernel $\exp(-|t - \mu(\lambda_i)|/\sigma)$, 4. Rayleigh kernel $(t\lambda_i)^{k-1} \exp(-(t\lambda_i)^2/2\theta^2)$, 5. t kernel $(1 + (t\lambda_i)^2/\theta)^{-(k+1)/2}$, 6. Inverse Chi square kernel $(t\lambda_i)^{-k/2-1} \exp(-\theta/2t\lambda_i)$.

This set of kernel functions are by no means exhaustive. We hope, however, it will illustrate the difference in between *coupled* and *decoupled* LFS. Note that HKS is a special case of Gamma kernel and WKS is a special case of Gaussian kernel.

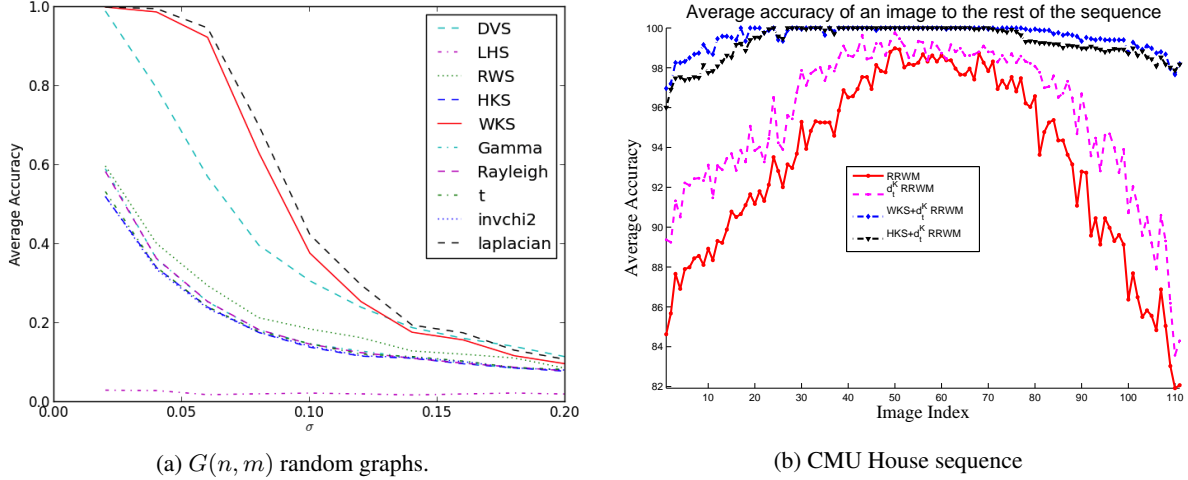


Figure 3: Matching Performance

We use bipartite matching as the matching scheme. In the experiment, we set $n = 50$ and m is uniformly in $[400, 1000]$, and generate 100 pairs of graphs. Fig. 3a shows the average accuracy¹ over the amount of noise added to the graph. As can be seen, *decoupled* LFS, WKS and Laplacian LFS, perform the best over all tested signatures. DVS performs the second tier, while *coupled* LFS, including HKS, Gamma LFS, Rayleigh LFS, t LFS and invchi2 LFS, are on the third tier, perform comparably with RWS. LHS is the worse in all tested signatures. This result validates our analysis on *coupled* and *decoupled* LFS, and the specific form of kernel $h(t; \lambda_k)$ seems less important than the coupling of parameters.

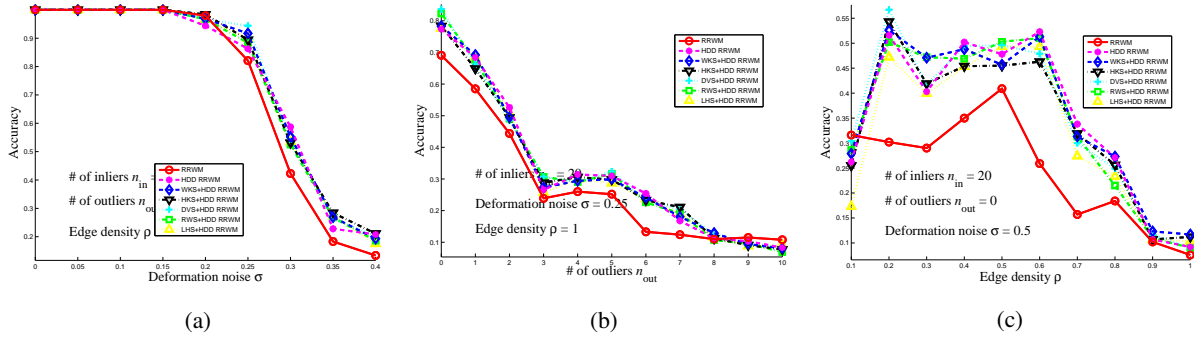


Figure 4: Matching accuracy of in the IQP setting. Note we used HDD in the legend of the figures to represent d_t^K .

In the second part of the experiment, we test different node signatures together with d_t^K as the pairwise constraint in the IQP setting. The random graphs are generated according to [?] (codes are publicly available). For a pair of graph

¹Accuracy is defined as the fraction of correct matches over ground truth matches.

G_1 and G_2 , they share n_{in} common nodes and $n_{\text{out}}^{(1)}$ and $n_{\text{out}}^{(2)}$ outlier nodes. Edge weights are randomly distributed in $[0, 1]$, and random Gaussian noise $\mathcal{N}(0, \sigma^2)$ are added.

In this experiment, we test the matching performance for W of i) only $d^A(i, j, a, b)$, ii) only $d_t^K(i, j, a, b)$, iii) $d_t^K(i, j, a, b)$ with different node signatures, on three different settings: 1. different level of deformation noise σ ; 2. different number of outliers; 3. different edge densities ρ . Fig. 4 showed the average matching accuracy. Red solid curve for RRWM is to match using pairwise adjacency distances d^A only as the baseline. With d_t^K substituting d^A , the matching performance is more noise tolerant. Comparing Fig. 3a and Fig. 4 (a), it can be seen that the large performance gap among node signatures, however, was marginalized out because of the second order compatibility constraint d_t^K . In Fig. 4 (c), the matching accuracy is much improved at different edge densities for a relatively large deformation noise ($\sigma = 0.5$).

4.2 CMU House Sequence

In this experiment, we use the CMU House sequence to test our descriptors. This sequence has been widely used to test different graph matching algorithms. It consists of 110 frames, and there are 30 feature points labeled consistently across all frames. We build fully connected graphs purely based on the geometry of the feature points, taking the Euclidean distance of the key points as the weights between pair of feature points. Affinity matrices W are set up similarly as in Section 4.1. We compute the average matching accuracy of each frame to the rest of frames in the sequence. Fig. 3b showed the accuracy of the matching. As can be seen the matching performance was improved when d_t^K is used to substitute d^A . With WKS as the first order compatibility, furthermore, the matching accuracy is much improved. Fig. 5 showed an example of the matching between the first and the last frame of the sequence (yellow lines are correct matches and red lines are wrong matches).

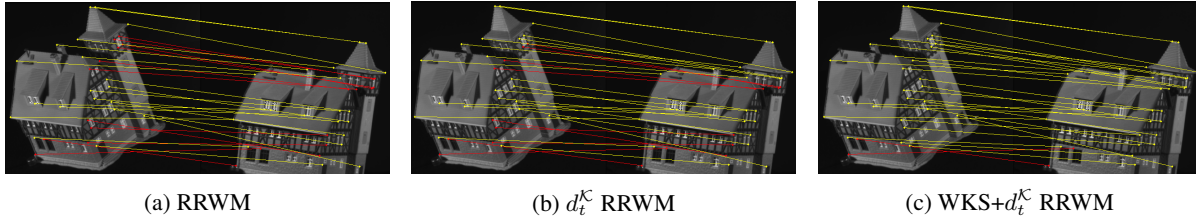


Figure 5: Matching on House sequence.

4.3 Real Image Feature Matching

In this experiment, we test our descriptor on the real image dataset used in [?]. This image dataset consists of 30 pairs of images with labeled feature points. In their original paper, affinity matrix W_{feat} is built considering the similarity between the appearance-based feature descriptors and the geometric transformations. Let $d_{\text{feat}}(i, j, a, b)$ be their compatibility functions. We put our spectral descriptors as additional structural compatibility, and set up the affinity matrix W as

$$W_{ia,jb} = \begin{cases} d_{\text{feat}}(i, j, a, b) + \alpha d_t^K(i, j, a, b) & i \neq j, a \neq b \\ \beta d(i, a) & i = j, a = b \end{cases}$$

Therefore, we could evaluate how our graph-based structural descriptors would improve the matching results. In our experiment, we tested different combination of α and β . If only considering d_t^K , $\beta = 0, \alpha = 1$ gives the best average accuracy, and by adding WKS as node signature constraint, $\alpha = 0.5, \beta = 4$ gives the best average accuracy. Table 1 listed the average accuracy as a comparison. Fig. 6 showed one example of matching results.

RRWM	d_t^κ RRWM	WKS+ d_t^κ RRWM
69.62	70.61	73.41

Table 1: Average accuracy of real image matching.

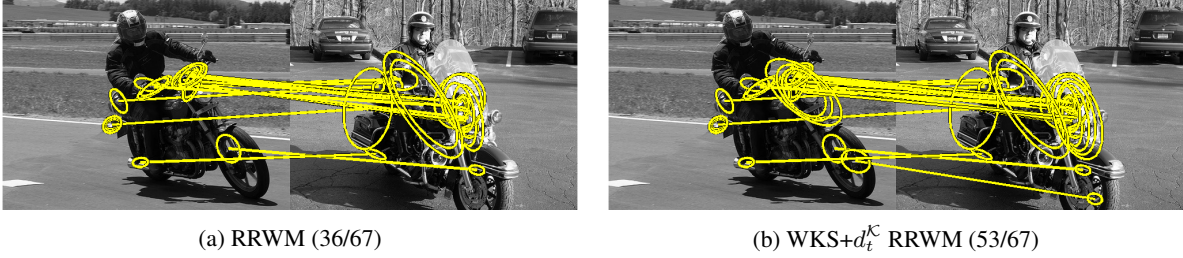


Figure 6: Matching on real images.

5 Conclusion

In this paper, we considered weighted graph matching problem. We propose to solve this problem in a IQP setting, where we use LFS and the pairwise heat kernel distance as the first and the second order constraint. We showed their properties that would benefit matching. In the experiment, we compared node signatures within LFS and with other existing ones, and found that the decoupling of parameters is crucial to the matching performance. Also, the combination of both compatibility functions increased the matching performance over the classical adjacency based compatibility.

Future work include pursuing the best signature within LFS from a learning perspective when some training dataset is given.

A Proof of Theorem 1 (LFS Continuity)

Theorem (LFS Continuity). *Let \mathcal{L} be the laplacian of a graph, and \mathcal{L}' be a perturbed laplacian. Let the size of the graph be n , and $\lambda_1 < \dots < \lambda_k$ denote the k distinct eigenvalues of \mathcal{L} . Let $s_i(t)$ and $s'_i(t)$ denote the LFS's of node i . If $\lambda_{j+1} - \lambda_j \geq \delta, \forall j$, $\|\mathcal{L} - \mathcal{L}'\|_F \leq \epsilon < \delta$, and $h(\cdot; \cdot) \in C^2(\mathbb{R}_+^2)$, then if $k = n$, we have*

$$|s'_i(t) - s_i(t)| \leq C_0(\delta, t)\epsilon,$$

where $C_0(\delta, t)$ is a constant independent of ϵ , and if $k < n$ we have

$$|s_i(t) - s'_i(t)| \leq C_1(t) \left(\frac{\delta}{\delta - \epsilon} - 1 \right) + C_2(t)\epsilon,$$

where $C_1(t), C_2(t)$ are constants depends only on t .

Proof of the first part of the theorem for non-repeated eigenvalues ($k = n$) requires the following theorems.

Theorem 3. [?] **(Sensitivity of Generalized Eigenvalues and Eigenvectors)** *Let K_0, M_0 be symmetric positive definite with distinct generalized eigenvalues λ_{0i} and generalized eigenvectors \mathbf{x}_{0i} , i.e. $K_0\mathbf{x}_{0i} = \lambda_{0i}M_0\mathbf{x}_{0i}$, $\forall i$, and $\mathbf{x}_{0i}^\top M_0 \mathbf{x}_{0j} = \delta_{ij}^j$, $\forall i, j$, where δ_{ij}^j is the Kronecker delta. If $K = K_0 + \Delta K$ and $M = M_0 + \Delta M$ are symmetric and positive definite, then the generalized eigenvalues λ_i and eigenvectors \mathbf{x}_i of $K\mathbf{x}_i = \lambda_i M\mathbf{x}_i$ satisfy*

1. $\lambda_i = \lambda_{0i} + \mathbf{x}_{0i}^\top (\Delta K - \lambda_{0i} \Delta M) \mathbf{x}_{0i}$.
2. $\mathbf{x}_i = \mathbf{x}_{0i} (1 - \frac{1}{2} \mathbf{x}_{0i}^\top \Delta M \mathbf{x}_{0i}) + \sum_{\substack{j=1 \\ j \neq i}}^N \frac{\mathbf{x}_{0j}^\top (\Delta K - \lambda_{0i} \Delta M) \mathbf{x}_{0i}}{\lambda_{0i} - \lambda_{0j}} \mathbf{x}_{0j}$.

Theorem 4. [?] (Maximum Eigenvalue) Let λ_{max} be the largest eigenvalue of a connected weighted graph G . Let $w(u, v)$ be the weight for edge (u, v) , and $d(v) = \sum_{u \neq v} w(u, v)$ the sum of incident weights. Then

$$\lambda_{max} \leq \max_{v \in V(G)} \left\{ d(v) + \frac{\sum_{u \neq v} w(u, v)d(u)}{d(v)} \right\}$$

Now let's prove the first part of the Theorem.

Proof. LFS Continuity For Non-Repeated Eigenvalues Laplacian eigenproblem is a special case of the generalized eigenproblem in Theorem 3. If we let $M_0 = I$, $\Delta M = 0$, and $\Delta K = \Delta \mathcal{L} \triangleq \mathcal{L} - \mathcal{L}'$. Let (λ_i, ϕ_i) , (λ'_i, ϕ'_i) be the eigenpairs of \mathcal{L} and \mathcal{L}' . By Theorem 3 we have,

$$\begin{aligned} \lambda'_i &= \lambda_i + \phi_i^\top \Delta \mathcal{L} \phi_i \\ \phi'_i &= \phi_i + \sum_{\substack{j=1 \\ j \neq i}}^N \frac{\phi_j^\top \Delta \mathcal{L} \phi_i}{\lambda_i - \lambda_j} \phi_j \end{aligned}$$

Note $\Delta \mathcal{L}$ is also a graph laplacian, and from Theorem 4, we have

$$\begin{aligned} \lambda_{max}(\Delta \mathcal{L}) &\leq \max_{v \in V(G)} \left\{ d(v) + \frac{\sum_{u \neq v} w(u, v)d(u)}{d(v)} \right\} \\ &\leq \max_{(u, v) \in E} \{d(u) + d(v)\} \leq |\Delta \mathcal{L}|_F < \epsilon \end{aligned}$$

Then, we have

$$\begin{aligned} |\lambda'_i - \lambda_i| &= |\phi_i^\top \Delta \mathcal{L} \phi_i| \leq \lambda_{max}(\Delta \mathcal{L}) < \epsilon \\ \|\phi'_i - \phi_i\|_2 &= \left\| \sum_{\substack{j=1 \\ j \neq i}}^N \frac{\phi_j^\top \Delta \mathcal{L} \phi_i}{\lambda_i - \lambda_j} \phi_j \right\|_2 \\ &\leq \frac{\lambda_{max}(\Delta \mathcal{L})}{\min(\lambda_i - \lambda_j)} \left\| \sum_{\substack{j=1 \\ j \neq i}}^N \phi_j \right\|_2 \leq \frac{\epsilon}{\delta} \end{aligned}$$

For $h(t; \cdot) \in C^2(\mathbb{R}_+^2)$, h has a Taylor expansion at λ_i

$$h(t; \lambda'_i) = h(t; \lambda_i) + h_i(t)(\lambda'_i - \lambda_i) + O(\Delta \lambda_i^2). \quad (1)$$

Plug (1) into $s_i(t)$ and ignoring higher order terms, we have

$$\begin{aligned} |s'_i(t) - s_i(t)| &= \left| \sum_k h(t; \lambda_k) \phi_k(i)^2 - \sum_k h(t; \lambda'_k) \phi'_k(i)^2 \right| \\ &\leq \left| \sum_k h(t; \lambda_k) (\phi_k(i)^2 - \phi'_k(i)^2) - \sum_k h_k(t) (\lambda'_k - \lambda_k) \phi'_k(i)^2 \right| \\ &\leq \frac{\max_k (h(t, \lambda_k)) 2|V|}{\delta} \epsilon + \max_k (h_k(t)) |V| \epsilon = C_0(\delta, t) \epsilon \end{aligned}$$

□

The proof to the second part of the theorem requires the following prerequisite.

Lemma 1 (Subspace Invariance of LFS). *Let \mathcal{L} be a graph laplacian, $\{\lambda_i\}$ are the eigenvalues of \mathcal{L} with multiplicity $\{k_i\}$. Suppose $\phi_{i1}, \dots, \phi_{ik_i}$, and $\phi'_{i1}, \dots, \phi'_{ik_i}$ are two sets of orthogonal eigenvectors corresponding to λ_i , $s_l(t)$ and $s'_l(t)$ are the LFS for node l computed using the two sets of eigenvectors respectively. Then, we have*

$$s_l(t) = s'_l(t), \forall l$$

Proof. For the case of eigenvalues with multiplicity, LFS of node l could be written as

$$s_l(t) = \sum_j h(t; \lambda_j) \sum_k \phi_{jk}(l)^2$$

WLOG, we only need to consider a specific λ_j with multiplicity k_j , and all we need to show is that $\forall l$, the following is true

$$\sum_{i=1}^{k_j} \phi_{ji}(l)^2 = \sum_{i=1}^{k_j} \phi'_{ji}(l)^2 \quad (2)$$

Note if we let $\Phi = [\phi_{j1}, \dots, \phi_{jk_j}]$, and $\Phi' = [\phi'_{j1}, \dots, \phi'_{jk_j}]$, (2) is equivalent to

$$\text{diag}(\Phi\Phi^\top) = \text{diag}(\Phi'\Phi'^\top)$$

As Φ and Φ' span the same subspace, Φ' can be expressed as a rotation (possibly reflection) and the permutation of Φ , i.e. $\exists R \in O^k$ and $P \in S^k$ a permutation matrix, such that $\Phi' = \Phi R P$. Hence, we have

$$\Phi'\Phi'^\top = \Phi R P P^\top R^\top \Phi^\top = \Phi\Phi^\top$$

□

Theorem 5. [?](Perturbation on Eigenvalues) *Let \mathcal{L} be the laplacian of a graph with n nodes, $\mathcal{L}' = \mathcal{L} + \Delta\mathcal{L}$ is a perturbed graph laplacian. If $\lambda_1 \leq \dots \leq \lambda_n$ and $\lambda'_1 \leq \dots \leq \lambda'_n$ are the eigenvalues to \mathcal{L} and \mathcal{L}' respectively. Then $\forall i$, we have*

$$|\lambda_i - \lambda'_i| \leq \|\Delta\mathcal{L}\|_2$$

Theorem 6. [?](Davis, Kahan sin theta theorem) *Let $A, A + H \in \mathbb{R}^{n \times n}$ be symmetric, $E_0, F_0 \in \mathbb{R}^{n \times k}$, $E_1, F_1 \in \mathbb{R}^{n \times (n-k)}$ where $E = [E_0 | E_1]$, $F = [F_0 | F_1] \in \mathbb{R}^{n \times n}$ are orthogonal basis of \mathbb{R}^n . Let*

$$\begin{aligned} A &= E \begin{pmatrix} A_0 & 0 \\ 0 & A_1 \end{pmatrix} E^\top, \\ A + H &= F \begin{pmatrix} B_0 & 0 \\ 0 & B_1 \end{pmatrix} F^\top. \end{aligned}$$

Let

$$d_p(E_0, F_0) \equiv \|E_0 E_0^\top - F_0 F_0^\top\|_2$$

If $\lambda(A_0) \subseteq [a, b]$, $\lambda(B_1) \subseteq (-\infty, a - \delta) \cup (b + \delta, \infty)$. Then

$$d_p(E_0, F_0) \leq \frac{1}{\delta} \|H\|_2.$$

Finally, we will have our continuity theorem on graph HKS.

Proof. LFS Continuity For Repeated Eigenvalues

Let d_i be the multiplicity of λ_i for $\forall i$, and $\{\phi_{i1}, \dots, \phi_{id_i}\}_i$ be the set of eigenvectors. Let $\lambda'_1 \leq \dots \leq \lambda'_n$ be the eigenvalues of L' and $\{\phi'_i\}$ be the corresponding eigenvectors. Clearly, we could rewrite $\{\lambda'_i\}$ as $\{\lambda'_{i1}, \dots, \lambda'_{id_i}\}_i$, and $\{v'_i\}$ as $\{\phi'_{i1}, \dots, \phi'_{id_i}\}_i$ for mathematical convenience. Then the difference on two LFS can be written as

$$\begin{aligned} |s_i(t) - s'_i(t)| &= \left| \sum_j \sum_k \left(h(t; \lambda_j) \phi_{jk}(i)^2 - h(t; \lambda'_{jk}) \phi'^2_{jk}(i) \right) \right| \\ &\leq \sum_j \left| \sum_k \left(h(t; \lambda_j) \phi_{jk}(i)^2 - h(t; \lambda'_{jk}) \phi'_{jk}(i)^2 \right) \right| \end{aligned}$$

Substituting (1) and ignoring higher order terms, we will have

$$\begin{aligned} &\left| \sum_k \left(h(t; \lambda_j) \phi_{jk}(i)^2 - h(t; \lambda'_{jk}) \phi'_{jk}(i)^2 \right) \right| \\ &\leq h(t; \lambda_j) \left| \sum_k \left(\phi_{jk}(i)^2 - \phi'_{jk}(i)^2 \right) \right| + h_j(t) \|\Delta \mathcal{L}\|_2 \sum_k v'^2_{jk}(i). \end{aligned}$$

The last term used the fact in Theorem 5. If we let $\Phi_j = [\phi_{j1}, \dots, \phi_{jd_j}]$ and $\Phi'_j = [\phi'_{j1}, \dots, \phi'_{jd_j}]$, and $\text{diag}(\cdot)_i$ be the i^{th} element of the diagonal of a matrix, we could rewrite

$$\begin{aligned} \left| \sum_k \left(\phi_{jk}(i)^2 - \phi'_{jk}(i)^2 \right) \right| &= \left| \text{diag}(\Phi_j \Phi_j^\top)_i - \text{diag}(\Phi'_j \Phi'^\top_j)_i \right| \\ &= \left| \text{diag}(\Phi_j \Phi_j^\top - \Phi'_j \Phi'^\top_j)_i \right| \\ &= \left| e_i^\top (\Phi_j \Phi_j^\top - \Phi'_j \Phi'^\top_j) e_i \right| \\ &\leq \left\| \Phi_j \Phi_j^\top - \Phi'_j \Phi'^\top_j \right\|_2 \\ &= \max_{\|x\|_2=\|y\|_2=1} x^\top (\Phi_j \Phi_j^\top - \Phi'_j \Phi'^\top_j) y \\ &= d_p(\Phi_j, \Phi'_j) \\ &\leq \frac{1}{\delta - \epsilon} \|\Delta \mathcal{L}\|_2 \end{aligned}$$

for $\epsilon < \delta$, where e_i is the standard vector. Note that $\|\cdot\|_2 \leq \|\cdot\|_F$, and summing over all j , we then have

$$\begin{aligned} |s_i(t) - s'_i(t)| &\leq \sum_j \left(h(t; \lambda_j) \frac{1}{\delta - \epsilon} \epsilon \right) + \sum_j h_j(t) \epsilon \\ &= C_1(t) \left(\frac{\delta}{\delta - \epsilon} - 1 \right) + C_2(t) \epsilon \end{aligned}$$

□

B Proof of Theorem 2 (Noise Tolerant Approximation)

Theorem (Noise Tolerant Approximation). *Let $d_t^{\mathcal{K}}(i, j, a, b)$ and $d^A(i, j, a, b)$ be the pairwise heat kernel distance and pairwise adjacency distance for graph G and G' . Let λ_i and λ'_i be the set of eigenvalues of G and G' .*

$$\lim_{t \rightarrow 0} \frac{d_t^{\mathcal{K}}(i, j, a, b)}{t} = d^A(i, j, a, b),$$

and

$$\sum_{i \neq j} \sum_{a \neq b} (d_t^{\mathcal{K}}(i, j, a, b))^2 \leq \sum_i \exp(-2t\lambda_i) + \sum_i \exp(-2t\lambda'_i)$$

Proof. Let $\mathcal{K}_t = \exp(-t\mathcal{L})$ be the matrix form of heat kernel, first order Taylor expansion will give

$$\mathcal{K}_t = I - t\mathcal{L} + O(t^2)$$

Therefore, for \mathcal{K}_t and \mathcal{K}'_t , we have

$$\begin{aligned} \mathcal{K}_t - \mathcal{K}'_t &= -t(\mathcal{L} - \mathcal{L}') + O(t^2) \\ &= -t(D - D') + t(A - A') + O(t^2). \end{aligned}$$

which is equivalent to

$$\lim_{t \rightarrow 0} \frac{d_t^{\mathcal{K}}(i, j, a, b)}{t} = d^A(i, j, a, b)$$

On the other hand,

$$\begin{aligned} \sum_{i \neq j} \sum_{a \neq b} (d_t^{\mathcal{K}}(i, j, a, b))^2 &\leq \|\mathcal{K}_t - \mathcal{K}'_t\|_F^2 \\ &\leq \|\mathcal{K}_t\|_F^2 + \|\mathcal{K}'_t\|_F^2 \\ &= \sum_k \lambda_k(\mathcal{K}_t)^2 + \sum_k \lambda_k(\mathcal{K}'_t)^2 \\ &= \sum_k \exp(-2t\lambda_k) + \sum_k \exp(-2t\lambda'_k) \end{aligned}$$

□